An Investigation of Mechanical and Thermal Properties of Polypropylene Reinforced with Different Clays

Alex S. Monteiro, Daili A. S. Barreira, Jaqueline S. Silva, Rene R. Oliveira, Francisco R. Valenzuela-Díaz and Esperidiana A. B. Moura

Abstract Nowadays, environmental awareness and an increasing concern with the greenhouse effect have increased the interest in composite materials containing at least one of the components from natural origin. Natural clays seem to be a good alternative because they are environmentally acceptable, naturally abundant minerals, and due to their ability to intercalate and exfoliate in the polymer matrix led to an improvement in mechanical, thermal and barrier properties, compared to the neat polymer. This work presents an investigation of the effects of incorporation of two different clays on mechanical and thermal properties of polypropylene (PP) matrix. PP with 1.5–3.0 wt% of the Cloisite® (commercial clay), and light green clay (non-commercial Brazilian clay), was prepared by melt extrusion process. The neat PP and its nanocomposites were characterized by mechanical tests, SEM, DSC, TGA and XRD analyses. In addition, clay characterization by XRD has also been carried out.

Keywords Light green clay · Cloisite® clay · Polypropylene · Tensile tests · TG DSC

A. S. Monteiro (✉) · D. A. S. Barreira · J. S. Silva · E. A. B. Moura
Nuclear and Energy Research Institute, Center for Chemical and Environmental Technology, 2242, Prof. LineuPrestes Av, São Paulo, SP 05508-000, Brazil
e-mail: montms@gmail.com

R. R. Oliveira
Nuclear and Energy Research Institute, Center for Materials Science and Technology, 2242, Prof. LineuPrestes Av, São Paulo, SP 05508-000, Brazil

F. R. Valenzuela-Díaz
Metallurgical and Materials Engineering Department, Polytechnic School, University of São Paulo, Prof. Mello de Moraes, 2463, São Paulo, PA 05508-030, Brazil

Introduction

The properties of polymers can be modified by the addition of fillers or fibers to meet specific requirements. In the last decades, the use of nanofillers (<100 nm) to reinforce polymers in order to enhance their properties for a variety of applications has attracted the attention from both industry and academia. Clay is among the most commonly used nanofillers for reinforcement of polymeric materials due to its availability, durability, and tailorable surface properties. Its characteristics lead to the improvement of polymer properties, with an addition of only one small amount (<5 wt%) and without requiring special processing techniques. The study of polymer–clay nanocomposites, also called as polymer-layered silicate nanocomposites is currently an expanding field of research because they frequently exhibit a wide range of improved properties over their neat polymers. The improved properties for polymer–clay nanocomposites include mechanical, thermal and flammability resistance, barrier properties, and electrical/electronic properties and other. The improvement of properties of polymer–clay nanocomposites is directly related to the complete exfoliation of silicate layers in the polymer matrix [1].

Several types of clays can be used to obtain polymer nanocomposites. The clays most commonly used are the ones from the smectite group, especially, the montmorillonite (MMT), a smectite clay that consists of octahedral aluminate sheet sandwiched between two tetrahedral silicate layers [2]. This clay is the most used as reinforcement in polymer because their silicate can be easily separated, or delaminated. Usually, in order to use the MMT clays in nanocomposites, the metallic cations are substituted by quaternary ammonium salts or other heteroatom organic salts. The method used to exchange the metallic cations by organic ones has a strong influence on the structure of the resultant organoclay [3].

One of the most widely used polymers is polypropylene (PP), due to its good combination of mechanical and thermal properties, lightweight, excellent mixture, heat and chemical resistance, favorable processing and recycle characteristics and relatively low price. The development of PP/clay nanocomposites has been much studied by scientists in recent years due to their promising compromise between properties and low cost in addition to traditional composites. The low clay loads that must be used to obtain the nanocomposite ensures the improvement of properties without the properties of the polymer (such as easy processability and lightweight) being affected [4].

This study aims to investigate the effects of the incorporation, by melt extrusion process, of the Cloisite®, a commercial clay, and light green clay a non-commercial Brazilian clay on the properties of polypropylene nanocomposites. However, due to the difference in their polarity, clays and polymers are nonmiscible, and therefore it is necessary to change the polarity of clay transforming it to the organophilic form that is more compatible with organic polymers and, thus, increases the capacity of the polymeric material to form exfoliated nanocomposites (desirable) [5]. The

extrusion process was used to prepare PP/clay nanocomposite in this study due to the relative simplicity of the process, the use of conventional polymer processing equipment, possibility of continuous and large-scale production, and consequently, more efficient and economical production from of the industrial viewpoint.

Materials and Methods

Materials

For the preparation of polypropylene/clay nanocomposites (PPCNs) the following materials were used. Polypropylene homopolymer H 301 with a melt flow index of 10 g/10 min (ASTM D 1238) and a density of 0.905 g/cm^3 (ASTM D 792) from Braskem S/A, clay Cloisite$^®$ Na$^+$one commercial clay from Southern clay products, and non-commercial Brazilian clay, the Light Green Clay (LGC) from Cubati, Paraiba, Brazil, chemically modified with a quaternary ammonium salt, Hexadecyl trimethylammonium chloride, purchased from BYK Additives and Instruments.

Light Green Clay Preparation

The modification process was an important step to obtain the organophilic clay. Initially, the RLGC was dispersed in deionized water in the ratio of 4 wt% with vigorous agitation for 30 min. After that, it was added Na$_2$CO$_3$ (50 meq of sodium per each 100 g of the RLGC) to replace the calcium ion in the RLGC. In the sequence, it was introduced a quaternary ammonium salt into the clay. Hexadecyl trimethylammonium chloride (70 meq of the quaternary ammonium salt) was introduced with vigorous agitation for 30 min. The organophilic light green clay (LGC) was decanted for 24 h, dried at 60 °C in an oven with air circulation for about 6 h and, finally, the LGC was milled to fine powder.

Nanocomposite Preparation

The PPNCs were prepared according to composition presented in Table 1 using a co-rotating twin-screw extruder "ZSK 18 Megalab" made by Coperion Werner and Pfleiderer GmbH & Co. The temperature profile was 175/180/185/190/195 °C. The screw speed was set from 20 to 30 rpm. The extrudate materials were cooled down in water at room temperature for a better dimensional stability, pelletized dried again at 60 ± 2 °C for 24 h and fed into injected molding where the temperature profile used

Table 1 PPCNs nanocomposites composition

Materials	PP (wt%)	LGC (wt%)	Cloisite® (wt%)
Neat PP	100	–	–
PP/LGC 1.5%	98.2	1.5	–
PP/LGC 3.0%	97.0	3.0	–
PP/Cloisite® 1.5%	98.5	–	1.5
PP/Cloisite® 3.0%	97.0	–	3.0

was 180/185/190/195 °C, and the mold temperature was set to 100 °C and specimens test samples were obtained.

Characterization Methods

Thermogravimetric Analyses (TG)

The TG of all samples were carried out using a Mettler Toledo TGA module, TGA/SDTA851e. To realize these analyses were weighed samples with 5.0 ± 0.5 mg of material. The temperature range was set from 25 to 600 °C with an increased rate of 10 °C/min, under nitrogen atmosphere (50 ml/min).

X-Ray Diffraction (XRD)

The XRD patterns of the light green clay and Cloisite® clay, the neat PP and PPCNs were obtained using Siemens—D5000 diffractometer operated at 40 kV and 40 mA, with copper Kα radiation($\lambda = 1.54$ Å) and 2θ varying between 2° and 50°. The interlayer spacing (d) of the clays were calculated through Bragg's Eq. 1 as given below:

$$n * \lambda = 2 d \operatorname{sen} \theta \tag{1}$$

where

n   whole number,
λ   1.54 Å is the incident radiation's wavelength,
d   interlayer spacing,
2θ   diffraction angle.

Differential Scanning Calorimetry (DSC)

The DSC experiments were performed with Mettler Toledo DSC 822e differential scanning calorimetry. All heating and cooling were carried out under a nitrogen condition atmosphere (50 ml/min) and using a temperature range from 25 to 250 °C with an increased rate of 10 °C/min. First, to remove previous thermal history, the materials were heated up to 250 °C (10 °C/min) and remained at that temperature for 5 min, and then were cooled to room temperature (10 °C/min). The samples were heated again to 250 °C with an increased rate of 10 °C/min and thus the melting temperature (Tm) and melting enthalpy (ΔHm) of neat PP and its composites were obtained. In addition, the crystallinity percentage variation (Xc) was calculated using Eq. 2, which is given below:

$$Xc = (\Delta Hm / \Delta Hm°(1 - w)) \times 100\%$$ (2)

where

Xc	percentage of crystallinity
ΔHm	melting enthalpy of the PPCNs,
ΔHm°	initial melting enthalpy of the PP assuming 100% crystallinity, 138 J/g,
W	mass fraction of the clay reinforcement in the materials.

Mechanical Tests

The tensile tests for all samples were performed according to ASTM D 638 using a Universal Testing Machine INSTRON, model 5564 at room temperature and loading rates of 50 mm/min.

Field Emission Scanning Electron Microscopy (FE-SEM)

FE-SEM of cryofractured samples under liquid nitrogen was carried out using a JEOL-JSM-6701 F, microscope with an accelerating voltage of 1–30 kV, using EDS Thermo-Scientific mod. Noran System Six software, in carbon sputtered samples.

Results and Discussion

Cloisite® and Light Green Clay Characterization

X-Ray Diffraction (XRD) Analysis

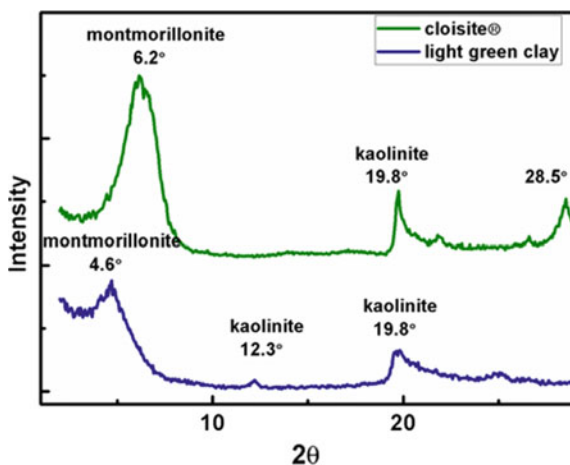The XRD pattern of Cloisite® and light green clay (LGC) are presented in Fig. 1.

Fig. 1 XRD pattern of the Cloisite® and original and modified light green clay (LGC)
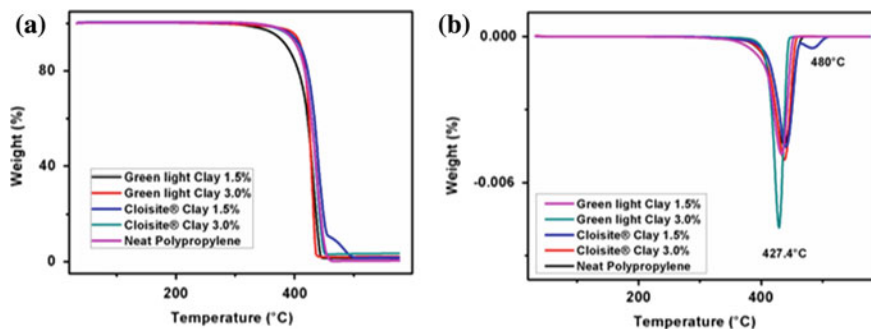

Fig. 2 Thermograms for the neat PP and PPCNs thermogravimetric (TG) (**a**), and DTG (**b**)

The XRD pattern of LGC presented three characteristic peaks: the montmorillonite peak, kaolinite peak ($2\theta = 12.3°$) and quartz peak ($2\theta = 26.6°$). By means of the XRD curves presented above, it can be observed that the original LGC exhibits a first 2θ peak at 5.5°, an interlayer distance (d_{001}) of 16.1 Å corresponding to montmorillonite, a second peak at 12.3° corresponding to kaolinite and the last peak at 26.6° corresponding to quartz. On the other hand, the modified LGC presented a shift for montmorillonite peak at 4.6° and an increase of (d_{001}) value to 19.2 Å. This increase confirms the intercalation of the quaternary ammonium cation in the interlamellar spacings of the LGC. As can be seen from Fig. 2, the 2θ peak at 26.6° corresponding to quartz of the original LGC increased the intensity after modification with quaternary ammonium salt.

Table 2 Decomposition temperatures and weight loss of PP and PPCNs

Materials	T_{onset} (°C)	$T_{máx}$ (°C)	Weight loss (%)
Neat PP	305	470	100
PP/LGC 1.5%	277	458	98.50
PP/LGC 3.0%	300	457	97.50
PP/Cloisite® 1.5%	307	508	98.50
PP/Cloisite® 3.0%	310	457	97.00

Neat PP and PPCNs Characterization

Thermogravimetric Analysis Results (TG)

Figure 2 shows the thermogravimetric (TG) (Fig. 2a) and derived thermogravimetric (DTG) (Fig. 2b) thermograms for the neat PP and PPCNs.

The decomposition temperatures and weight loss of the neat PP and its nanocomposites are presents in Table 2.

It is possible to observe that it presented two thermal events and presented a thermal stability up to approximately 400 °C. From this temperature, the beginning of the thermal degradation was observed with the first event occurring in a temperature range of 450–470 °C, this being the largest event observed with loss of 90% of the initial weight of the sample, and second peak is about 500 °C. Thermal analysis of neat PP and nanocomposites confirms the slower decomposition rate of the composites compared to the pure polymer. The rate of decomposition as a function of temperature of the PP/LGC 1.5 wt% and PP/Cloisite® 1.5 wt% was similar, but for the PP/Cloisite® 3.0 wt% charge proportion the rate was decreased.

TG and DTG analysis of the thermal stability of the sample's determination provided the information, from of the decomposition temperature of the PP/nanocomposite clays, that for all the composite samples the thermal degradation was complete above 450 °C.

Differential Scanning Calorimetry (DSC)

Figure 3 shows DSC melting curves for 2° heating cycle of neat PP and their PP/clay nanocomposites. It can be seen in this figure, a reduction in melting enthalpy and consequently in crystallinity percentage of neat PP due to both LGC and Cloisite® clays addition. In relation to the melting temperature, the results have shown a slight reduction for the addition of the 1.5 wt% of clays, but when clays addition into PP increases to 3.0 wt%, the melting temperature of all nanocomposites tends to increase also.

Table 3 presents the values of melting temperature and enthalpy, and the crystallinity percentage of neat PP, PP/LGC and PP/Cloisite® nanocomposites.
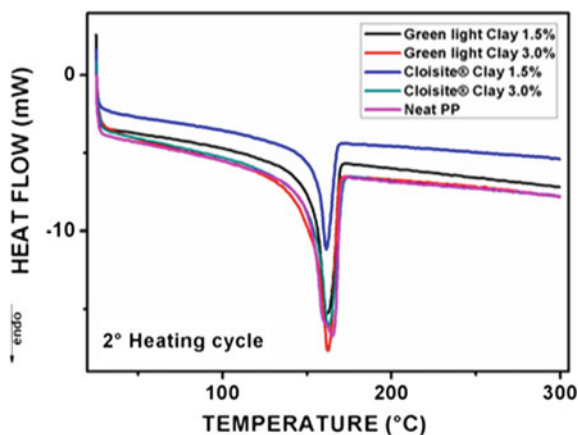
Fig. 3 DSC melting curves of

Table 3 Melting temperature and enthalpy, and crystallinity percentage of neat PP, PP/LGC and PP/Cloisite®

Materials	Melting temperature (T$_m$ °C)	Melting enthalpy (ΔHm J g^{-1})	Crystallinity percentage (Xc %)
Neat PP	164.9	94.40	68.70
PP/LGC (98/1.5 wt%)	163.9	81.98	52.90
PP/LGC (97/3.0 wt%)	166.8	78.55	51.25
PP/Cloisite® (98/1.5 wt%)	164.7	82.80	53.50
PP/Cloisite® (97/3.0 wt%)	165.2	80.87	51.75

X-Ray Diffraction (XRD) Analysis

The XRD pattern of neat PP, PP/LGC and PP/Cloisite® are presented in Fig. 4. Neat PP presented three characteristics peaks: $2\theta = 14°$ referring to crystalline plane (110), $2\theta = 16.8°$ referring to crystalline plane (040) and $2\theta = 18.4°$ referring to crystalline plane (130). Analysing Fig. 4, it can be observed that none of the PP's nanocomposites exhibited reminiscent basal peak of its respective organoclays ($2\theta = 4.6°$ to LGC and $2\theta = X°$ to Cloisite®). The XRD peaks that appear to all PP nanocomposites have the same diffraction angle (2θ) of the neat PP peaks, the difference is only the intensity of this peaks, indicating that PP chains have diffused into the layer of both clays and the clays were successfully intercalated in the PP matrix; in other words, these results suggest a formation of intercalated structure.
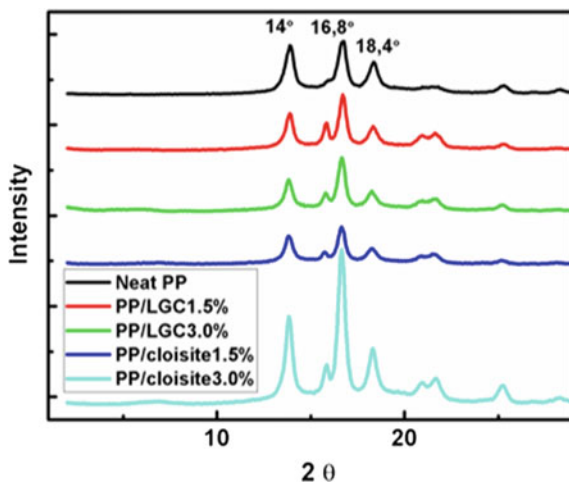
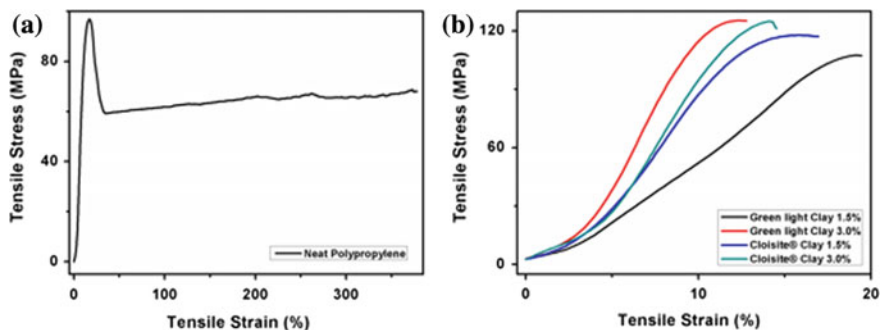**Fig. 4** XRD pattern of neat PP, PP/LGC and PP/Cloisite[®]

Fig. 5 Diagram stress (MPa) X strain (%) for tensile tests of the neat PP (**a**); PP/LGC and PP/Cloisite[®] (**b**)

Mechanical Properties

Figure 5 shows the diagram stress (MPa) X strain (%) for tensile tests of the neat PP (5A); PP/LGC and PP/Cloisite[®] (5B). The results presented show the average values calculated from the data obtained in tests for five test specimens. As can be seen in Fig. 5, the addition of both LGC and Cloisite[®] into PP matrix led to an important increase in tensile strength and Young's modulus of PP matrix.
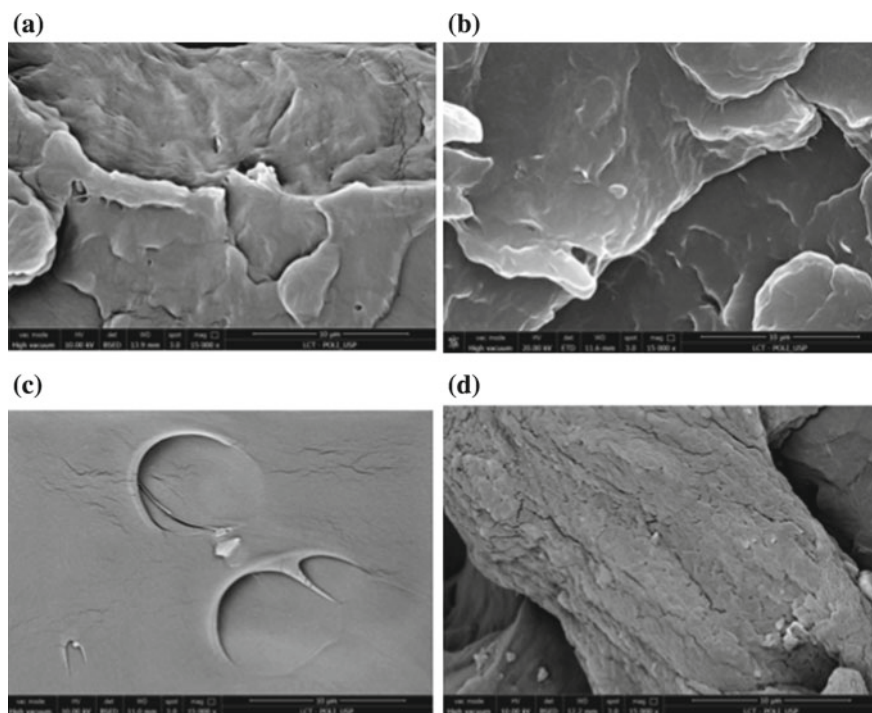
Fig. 6 FE-SEM micrographs for all PP nanocomposites; **a** PP/LGC1.5%; **b** PP/LGC3.0%; **c** PP/Cloisite® 1.5% and **d** PP/Cloisite® 3.0%

Field Emission Scanning Electron Microscopy (FE-SEM)

FE-SEM micrographs of cryofractured surfaces of the PP/LGC and PP/Cloisite® nanocomposites are shown in Fig. 6. These micrographs were studied to understand the interactions between the clays and PP matrix. As expected, the nanocomposites with major quantity of clay (PP/LGC 3.0% and PP/Cloisite® 3.0%) presented more clusters of clay dispersed. However, as it can be seen in this figure, all nanocomposites obtained shows a rough cryofractured surfaces with few clusters of clay dispersed, suggesting a good dispersal of the clay in matrix according to XRD results.

Conclusions

All of the results pointed out that all nanocomposites presented a good interfacial interaction between the matrix and both clays and superior mechanical properties when compared with neat PP. The tensile strength of the PP/Cloisite® 3.0 wt% and PP/LGC 3.0 wt% nanocomposites showed an increment of about 23% over tensile strength of neat PP.

References

1. Alexandre M, Dubois P (2000) Polymer-layered silicate nanocomposites: preparation, properties and uses of a new class of materials. Mater Sci Eng Rep 28:1–63
2. Modak SK, Mandal A, Chakrabarty D (2013) Studies on synthesis and characterization of poly(methyl methacrylate)-bentonite clay composite by emulsion polymerization and simultaneous in situ clay incorporation. Polym Compos 34:32–40
3. Delbem MF, Valera TS, Valenzuela-Diaz FR, Demarquette NR (2010) Modification of a brazil-iansmectite clay with different quaternary ammonium salts. Quim Nova 33(2):309–315
4. Le Pluart L, Duchet J, Sautereau H, Gerard JF (2002) Surface modifications of montmorillonite for tailored interfaces in nanocomposites. J Adhesion 78:645–662
5. Morgan AB, Gilman JW (2003) Characterization of polymer layered silicate (clay) nanocomposites by transmission electron microscopy and X ray diffraction: a comparative study. J Appl Polym Sci 87:1329–1338
6. Favaro MM, Branciforti MC, Bretas RES (2009) A X-ray study of β-phase and molecular orientation in nucleated and non-nucleated injection molded polypropylene resins. Mat Res 12:455–464